Supporting Information

Concerted interactions between multiple gp41 trimers and the target cell lipidome may be required for HIV-1 entry

Biswajit Gorai, Anil Kumar Sahoo, Anand Srivastava, Narendra M. Dixit, and Prabal K. Maiti

[a]Center for Condensed Matter Theory, Department of Physics, Indian Institute of Science, Bangalore-560012, India; [b]Molecular Biophysics Unit, Biological Sciences Division, Indian Institute of Science, Bangalore-560012, India; [c]Department of Chemical Engineering, Indian Institute of Science, Bangalore-560012, India; [d]Centre for Biosystems Science and Engineering, Indian Institute of Science, Bangalore-560012, India.

[!]Current Address: Department of Chemical Engineering, University of New Hampshire, 33 Academic Way, Durham, NH 03824.

[@]Current Address: Biomaterials Department, Max Planck Institute of Colloids and Interfaces, 14476 Potsdam, Germany, Fachbereich Physik, Freie Universität Berlin, 14195 Berlin, Germany.

*To whom correspondence should be addressed: maiti@iisc.ac.in

This PDF file includes:

Figures S1 to S12
Table S1 to S4
Caption for Movie S1

Other supplementary materials for this manuscript include the following:

Movie S1

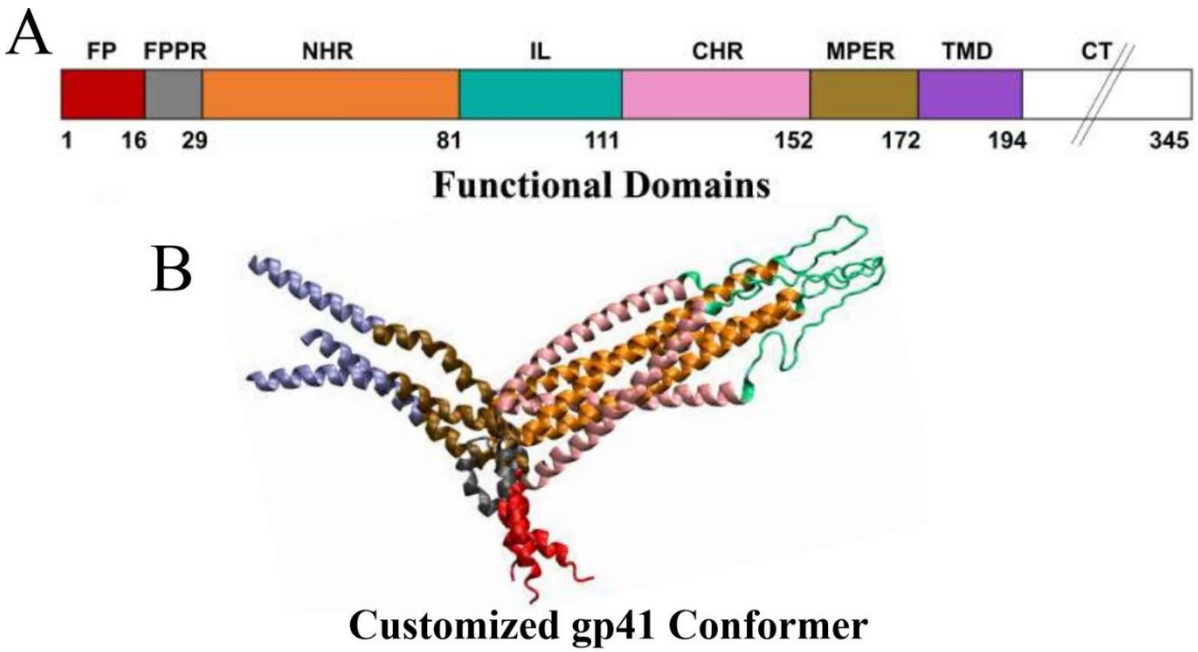

Figure S1. The functional domains and splayed conformer of HIV-1 gp41. (A) Different colored bars are used to represent fusion peptide (FP), fusion peptide proximal region (FPPR), N-terminal heptad repeat (NHR), immunodominant loop (IL), C-terminal heptad repeat (CHR), membrane-proximal external region (MPER), transmembrane domain (TMD), and cytoplasmic domain (CD). The cartoon representaion of trimer of the HIV-1 gp41 TMD-ectodomain region (residues 1–194), used in the current study, is shown. The conformer is generated after splaying the FP+FPPR and MPER+TMD of modelled post fusion conformer of gp41 trimer, taken from our previous study (refer main text for reference), in opposite direction.

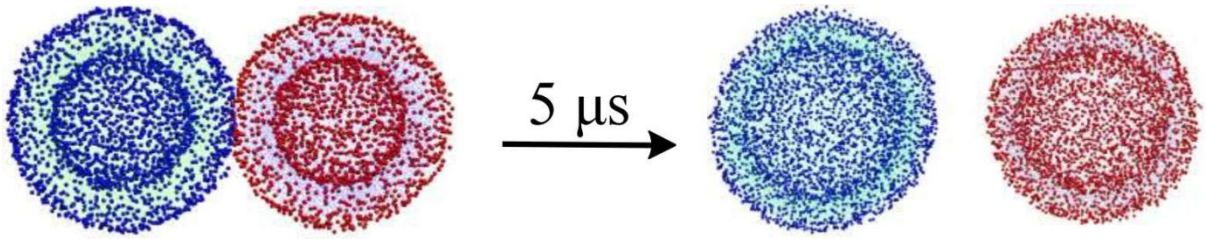

Figure S2. Simulation of the human and HIV-1 vesicle membrane models, with near biological compositions, in the absence of gp41. The initial (left) and final (right) configurations of the simulated system at 300 K containing the human and HIV-1 vesicles without any gp41 trimer are shown. The lipid head groups and tails of the human vesicle are shown in vdW (blue) and line (green) representations, respectively. The lipid head groups and tails of the HIV-1 vesicle are shown in vdW (red) and line (light blue) representations, respectively. Water and ions are not shown here for clarity.

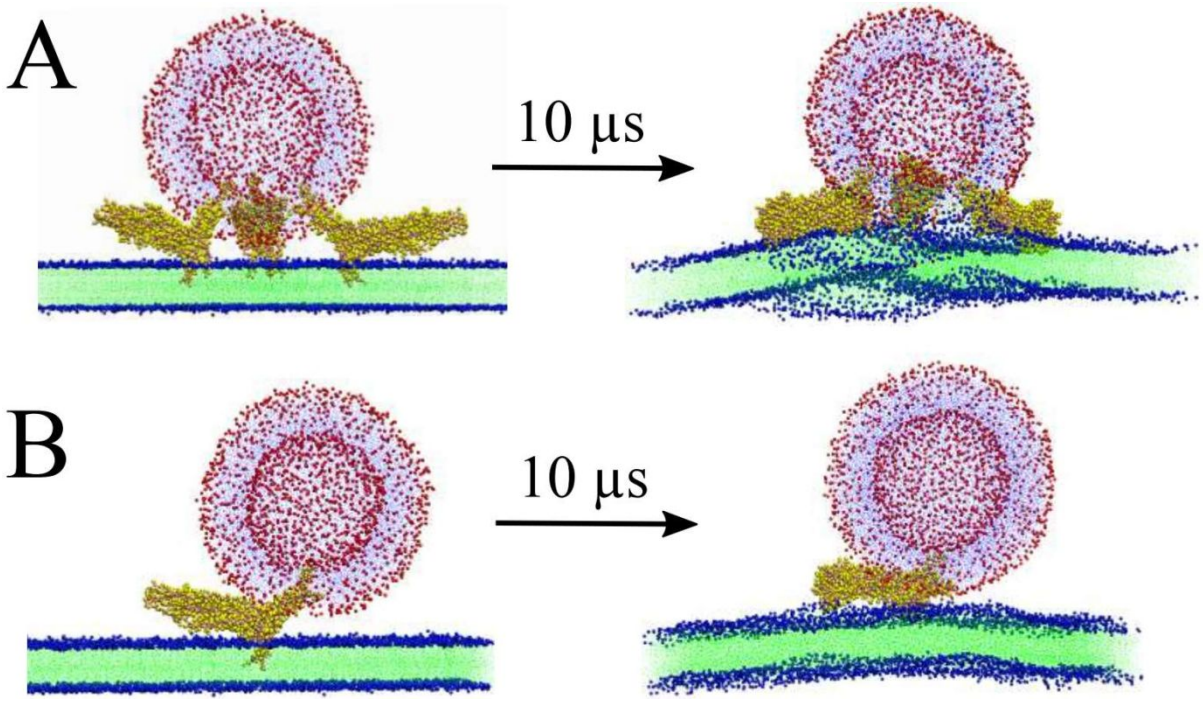

Figure S3. Simulation of the human and HIV-1 membrane models, with near biological compositions, in the presence of gp41. The initial (left) and final (right) configurations of the simulated system at 300 K consisting of the human bilayer and HIV-1 vesicle in the presence of (A) triple and (B) single gp41 trimeric units are depicted. The lipid head groups and tails of the human bilayer are shown in vdW (blue) and line (green) representations, respectively. The lipid head groups and tails of the HIV-1 vesicle are shown in vdW (red) and line (light blue) representations, respectively. The gp41 trimeric unit is shown in vdW representation with yellow color. Water and ions are not shown here for clarity.

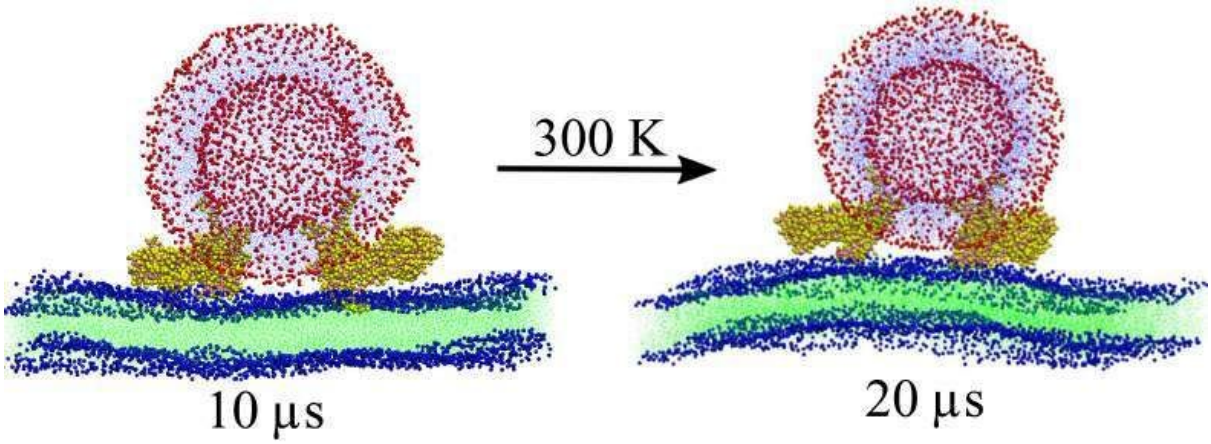

Figure S4. Extension of simulation of the human and HIV-1 membrane models in the presence of 2 gp41 trimers. The configurations of the simulated system at 300 K at 10 μs (left) and at 20 μs (right) consisting of the human bilayer and HIV-1 vesicle in the presence of double gp41 trimeric units are depicted. The lipid head groups and tails of the human bilayer are shown in vdW (blue) and line (green) representations, respectively. The lipid head groups and tails of the HIV-1 vesicle are shown in vdW (red) and line (light blue) representations, respectively. The gp41 trimeric unit is shown in vdW representation with yellow color. Water and ions are not shown here for clarity.

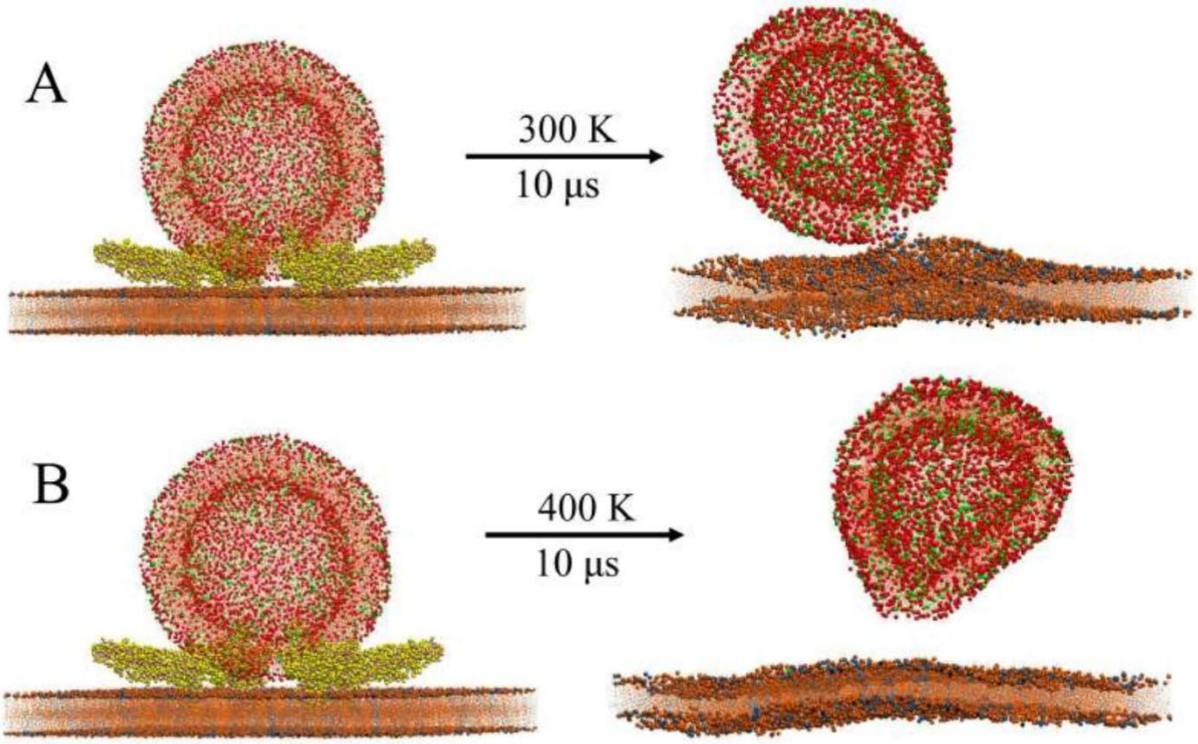

Figure S5. Simulation of the human and HIV-1 membrane models, with arbitrary lipid compositions, in the presence of gp41. The snapshots of the initial (left) and final (right) configurations of the human bilayer and HIV-1 vesicle composed of POPC and POPS in 80:20 proportion at (A) 300 K, and (B) 400 K for 10 μs are shown. The POPC and POPS lipids of the human bilayer are shown in brown and blue colors, respectively. The POPC and POPS lipids of the HIV-1 vesicle are shown in red and green colors, respectively. The gp41 trimer is depicted in yellow vdW representations. The exchange of lipids between human and HIV-1 cell membranes with non-biological compositions at room temperature, as well as elevated temperatures are not observed. This observation justifies the complex composition adapted by the cell membranes to accomplish the critical biological phenomenon. The gp41 in the final configuration, water and ions are not shown here for clarity.

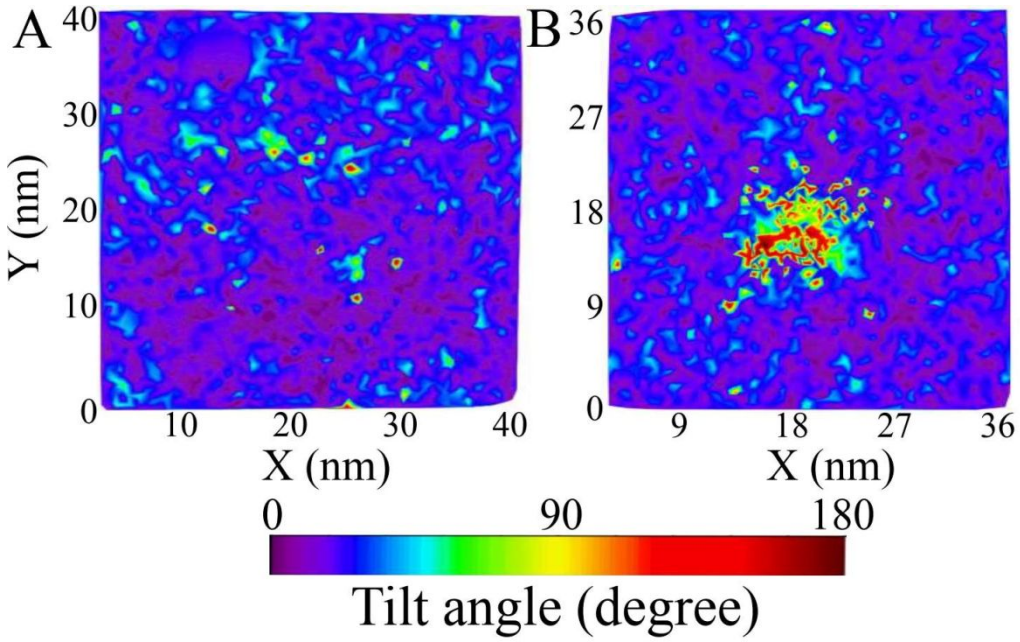

Figure S6. Lipid tilt distribution map. The surface distribution of tilt angle of lipids of the human bilayer at (A) the beginning of simulation, and (B) at beginning of stalk formation is shown. The variation in the tilt angle of the lipids can be estimated from the color scale beneath the figure.

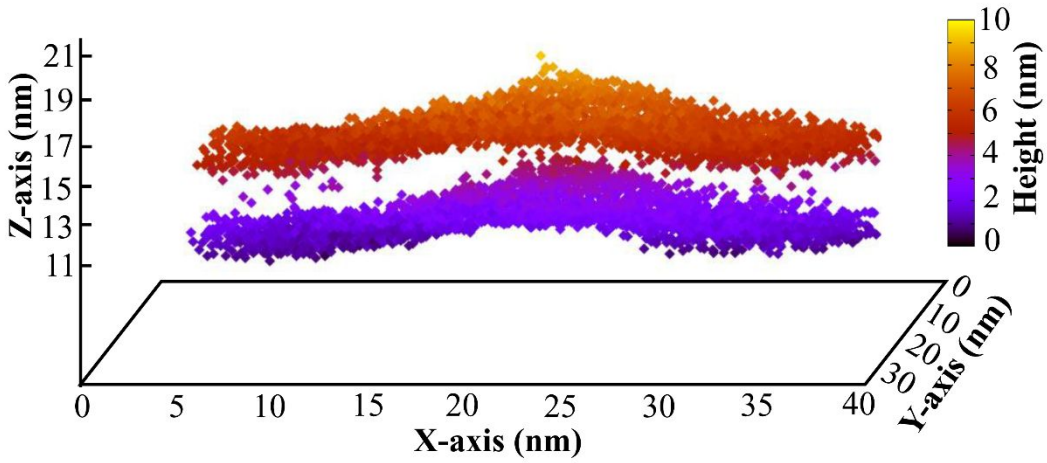

Figure S7. Morphology of human cell membrane during stalk initiation. The 3D projection map (with X-, Y- and Z-axis) of head groups of lipids (represented by colored squares) of human cell membrane is shown in the figure. The normalized height of the lipid heads is represented by different colors as quantified by the color scale on the right of the figure.

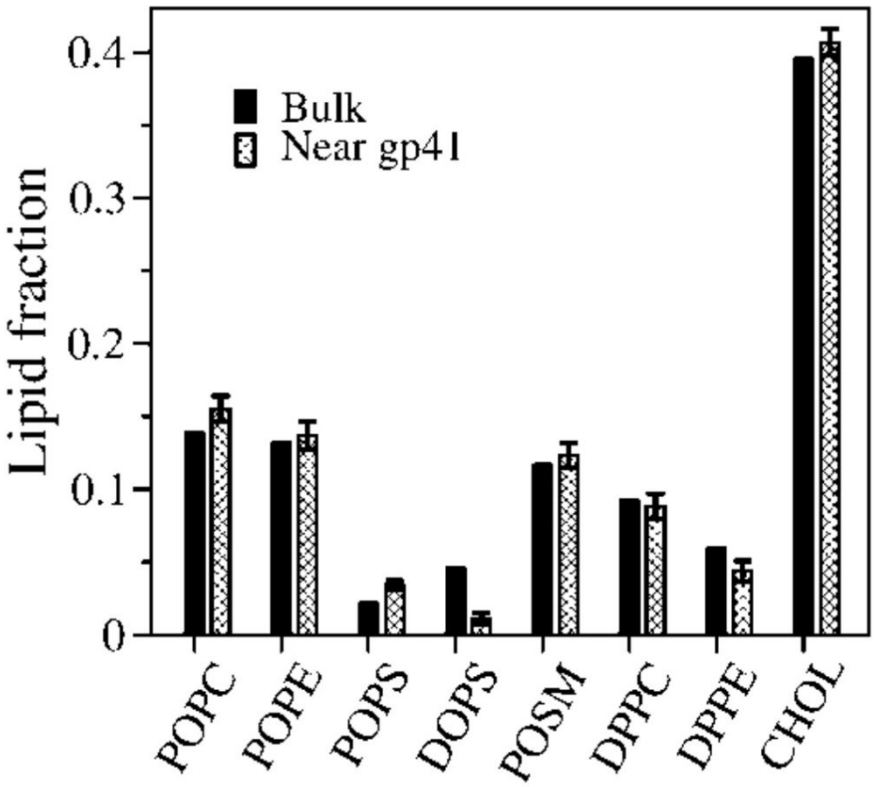

Figure S8. Histogram plot of lipid fractions. Fraction of each lipids at the bulk (not within 20 Å of center of mass of gp41 FP+TMD domain) and near gp41 trimeric units (within 20 Å of center of mass of gp41 FP+TMD domain) calculated during the simulation time is shown.

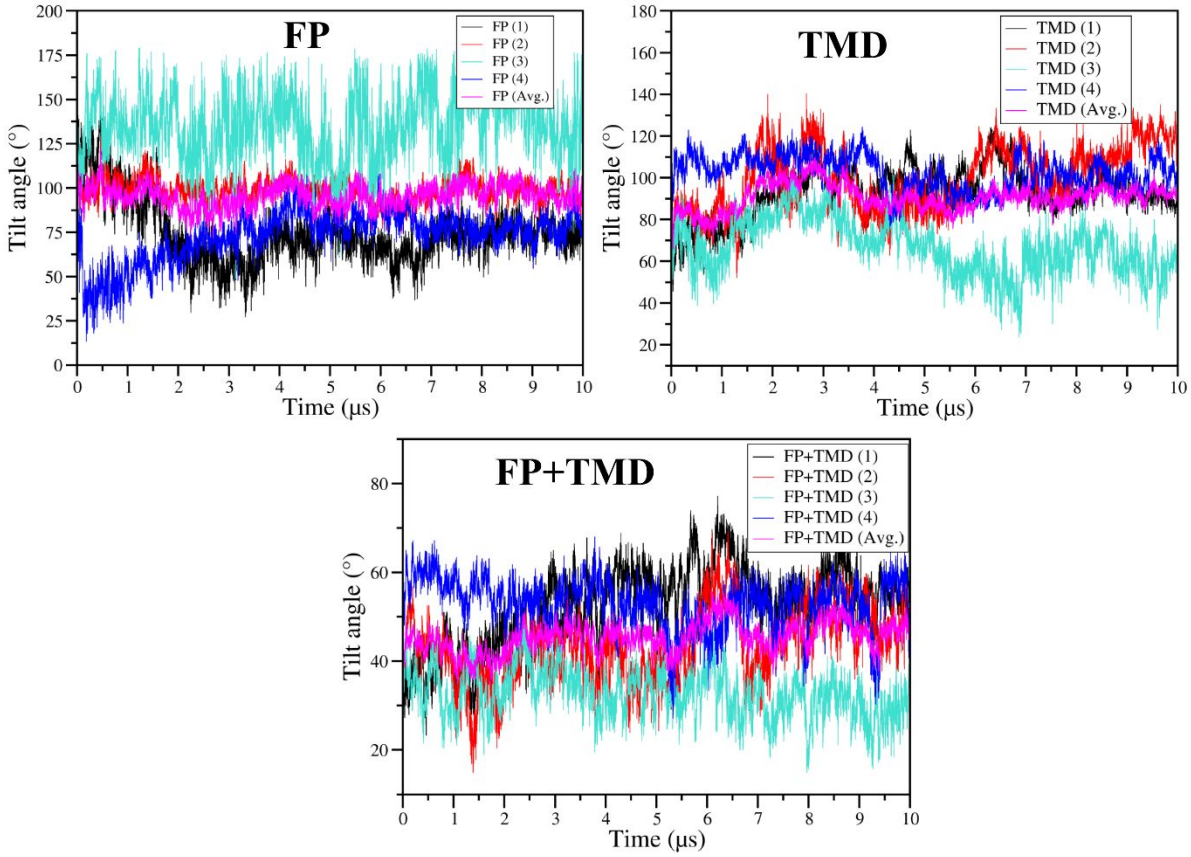

Figure S9. Tilt angle of gp41 functional domains. The tilt angle of FP, TMD and FP+TMD domains with the simulation time is shown in the figure. The tilt angle of units 1 to 4 and their average are depicted in distinct colors as depicted in the figure legend box.

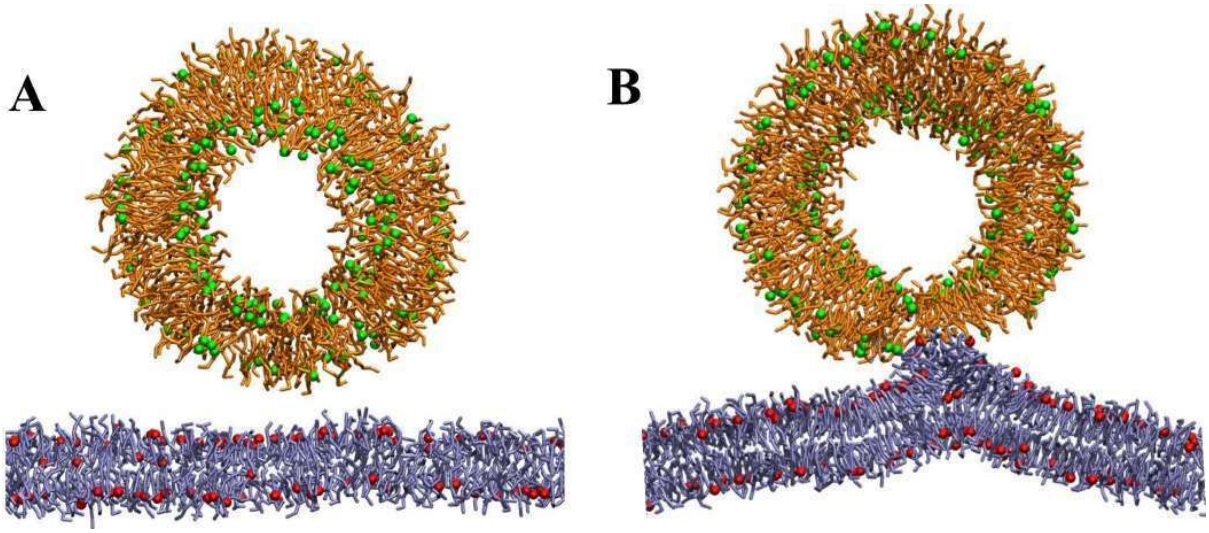

Figure S10. Stalk initiation snapshot. The clipped image of the (A) initial and (B) stalk initiation stage during simulation of HIV-1 and human bilayer using 4 gp41 trimers at 300 K is depicted. The HIV-1 and human membrane models are represented by vesicle and bilayer, respectively. Water, ions and gp41 units are not shown here for the clarity.

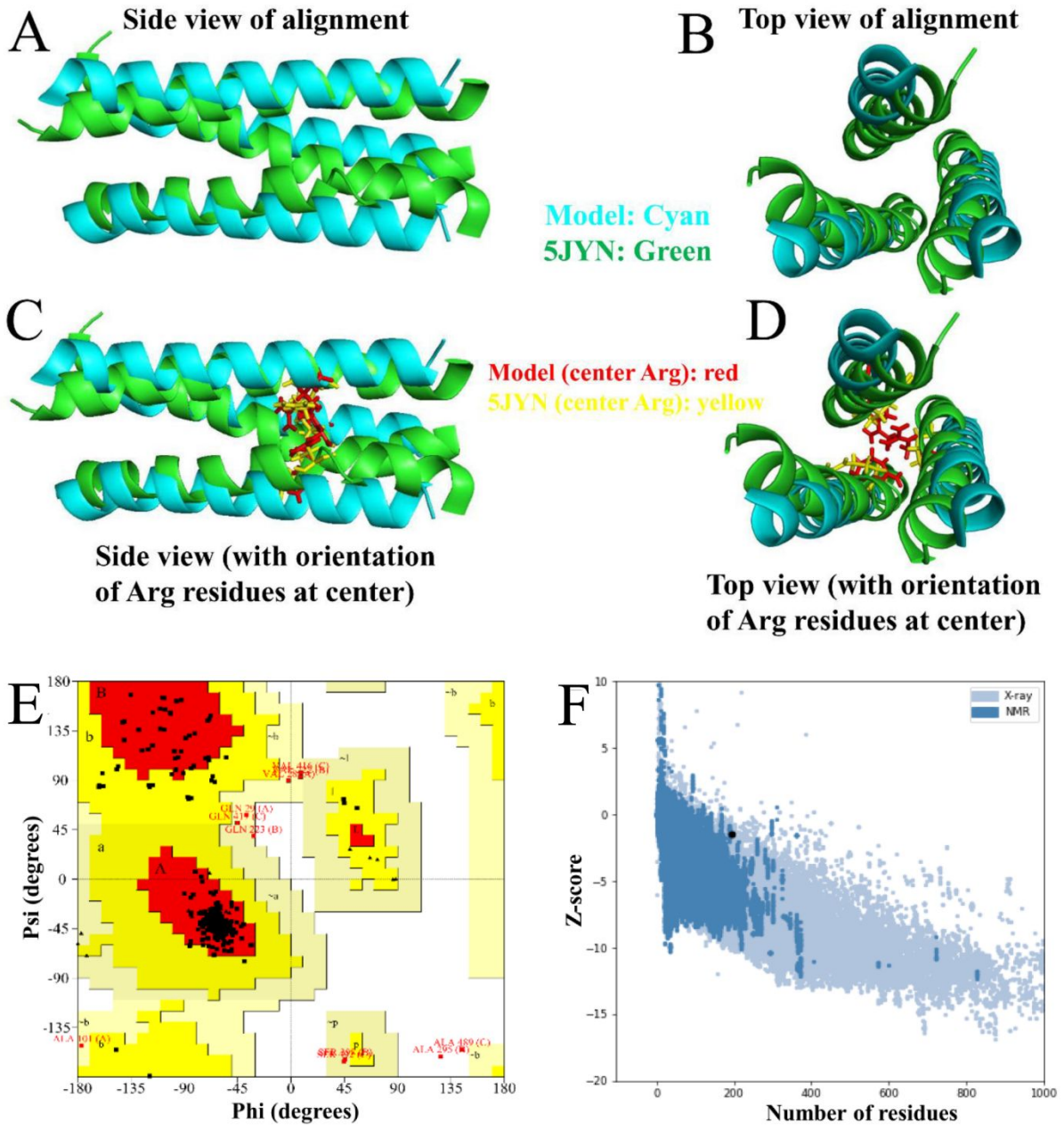

Figure S11. Structural superimposition of modelled structure (cyan) with the available experimental structure (green) and quality assessment. The side (A) and top (B) view of structurally aligned structures is depicted in the figure. The side (C) and top (D) view of aligned arginine residues at the center of the modelled structure (red) and experimental structure (yellow) in stick representation is shown here. (E) The Ramachandran plot analysis of the modelled structure shows the distribution of dihedral angles (Phi and Psi) of the non-proline and non-glycine residues. (F) The z-score value of the modelled structure is represented by a black dot in the ProSA plot.

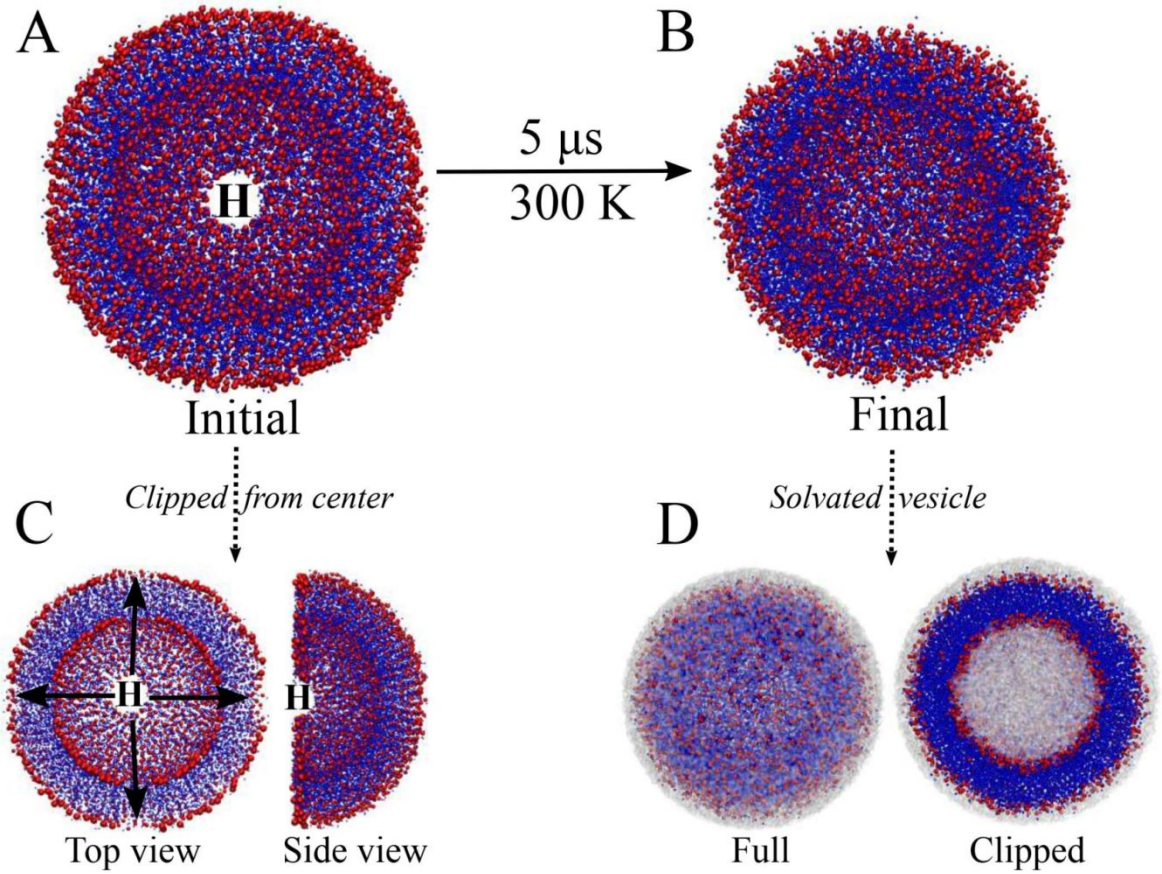

Figure S12. Equilibration of HIV-1 vesicle. Initially, the HIV-1 vesicle obtained from CHARMM-GUI web server contains (A) 6 holes (H). (C) The location of holes are shown in the top and side view of HIV-1 vesicle, clipped from the center. The initial structure was subjected to CGMD equilibration and production run to obtain a (B) stable vesicle without holes. The stable HIV-1 vesicle, with (D) a water layer (surface representation) of around 11 nm radius from the center of the vesicle is used for further fusion study. The lipid head groups and tails of the HIV-1 vesicle are shown in vdW (red) and dots (blue) representations, respectively. The simulation was performed in the presence of ions and explicit coarse-grained water model, but not shown in (A) and (B) for clarity.

Table S1. Lateral diffusion of human bilayer lipids before and after stalk formation

Lipid	MSD* before stalk (0 -1.5 μs)	MSD* after stalk (1.5 - 3 μs)
i) Chol	3.1±0.25 x 10^{-7} cm^2/s	3.4±0.25 x 10^{-7} cm^2/s
ii) DOPS	2.4±0.03 x 10^{-7} cm^2/s	2.7±0.03 x 10^{-7} cm^2/s
iii) DPPC	2.6±0.6 x 10^{-7} cm^2/s	2.8±0.15 x 10^{-7} cm^2/s
iv) DPPE	2.9±0.05 x 10^{-7} cm^2/s	2.9±0.5 x 10^{-7} cm^2/s
v) POPC	2.2±0.12 x 10^{-7} cm^2/s	2.6±0.36 x 10^{-7} cm^2/s
vi) POPE	2.1±0.5 x 10^{-7} cm^2/s	3.64±0.05 x 10^{-7} cm^2/s
vii) POSM	0.7±0.16 x 10^{-7} cm^2/s	1.3±0.06 x 10^{-7} cm^2/s
viii) Human bilayer	2.6±0.05 x 10^{-7} cm^2/s	3.1±0.34 x 10^{-7} cm^2/s

*Note: To compare the diffusion coefficient obtained from a Martini simulation to a measured one, a conversion factor of about 4 has to be applied to account for the faster diffusion at the CG level due to the smoothened free energy landscape.

Table S2: The error in initiation time at each simulation temperature with 4 gp41 trimers

Sl. No.	Temperature (K)	Initiation time (μs)		Average ± Std. dev. (μs)
		Run1	Run2	
1	300	1.43	1.33	1.38 ± 0.05
2	320	1.15	1.25	1.2 ± 0.05
3	340	0.53	0.5	0.515 ± 0.015
4	360	0.43	0.47	0.45 ± 0.02
5	400	0.108	0.102	0.105 ± 0.003

Table S3. **Details of the contact time at different temperatures and ΔG_S, with 3 and 4 gp41 trimer units**

Temp (K)	Avg. contact time (μs) with 3 gp41	Avg. contact time (μs) with 4 gp41
300	1.63 ± 0.24	1.38 ± 0.05
320	1.26 ± 0.13	1.20 ± 0.05
340	n.a.*	0.52 ± 0.02
360	0.61 ± 0.13	0.45 ± 0.015
400	0.11 ± 0.0	0.105 ± 0.003
ΔG_S	6.2 ±1.47 kcal/mol	6.16 ±1.0 kcal/mol

*n.a.- Data not available, as simulation was not performed at 340 K with 3 gp41 trimers

Table S4. The lipid composition of HIV-1 cell membrane and human T-cell membrane.

Sl. No.	Lipid	HIV-1		Human	
		IL	OL	IL	OL
1	DPPC	0	0	208	591
2	DPPE	0	0	176	335
3	DOPS	0	0	389	0
4	POPC	64	223	643	279
5	POPE	313	211	155	460
6	POPS	153	34	0	0
7	POSM	66	524	306	117
8	CHOL	609	726	1079	1088

The membranes are composed by dipalmitoyl phosphatidylcholine (DPPC), dipalmitoyl phosphatidylethanolamine (DPPE), dioleoyl phosphoserine (DOPS), palmitoyl oleoyl phosphocholine (POPC), palmitoyl oleoyl phosphatidylethanolamine (POPE), palmitoyl oleoyl phosphoserine (POPS) palmitoyl oleoyl sphingomyelin (POSM), and cholesterol (CHOL). The lipid composition of HIV-1 and human T-cell membranes are highly inhomogeneous, with asymmetric inner leaflet (IL) and outer leaflet (OL) lipid composition.

Movie S1. Human–HIV-1 inter-membrane lipid transfer. The transfer of lipids from the human bilayer (left) to HIV-1 vesicle (right) during 10 μs CGMD simulation time at 300 K in presence of quadruple gp41 trimers is shown. The human and HIV-1 membranes are from the same simulation system. Different lipid types are represented in distinct colors. Water, ions, and gp41 trimers are not shown in the video for clarity.